CHAPTER 11

# *Nuclear Structure*

**Contents**



Throughout the ages and in every civilization, people have developed explanations of observed behaviors. These explanations are based on the principle of causality, i.e. every effect has a cause and the same cause produces always the same effect. We call these explanations *models*.

Scientists are professional model-builders. Observed phenomena are used to develop a model, which then is tested through new experiments. This is familiar to every chemist: although we cannot see the atoms and molecules which we add into a reaction vessel, we

certainly have some idea about what is going to happen. It is indeed our enjoyment in developing models which causes us to experiment in science. We also want to be able to make quantitative predictions based on our models which we therefore formulate in mathematical terms. To allow tractable calculations most models involves simplifications of the "real world". Of course, since man is fallible some models may turn out to be wrong but as new data accumulate, wrong or naive models are replaced by better ones.

We have already shown how one model for the nuclear structure, the liquid drop model, has helped us to explain a number of nuclear properties, the most important being the shape of the stability valley. But the liquid drop model fails to explain other important properties. In this chapter we shall try to arrive at a nuclear model which takes into account the quantum mechanical properties of the nucleus.

## 11.1. Requirements of a nuclear model

Investigation of light emitted by excited atoms (J. Rydberg 1895) led N. Bohr to suggest the quantized model for the atom, which became the foundation for explaining the chemical properties of the elements and justifying their ordering in the periodic system. From studies of molecular spectra and from theoretical quantum and wave mechanical calculations, we are able to interpret many of the most intricate details of chemical bonding.

In a similar manner, patterns of nuclear stability, results of nuclear reactions and spectroscopy of radiation emitted by nuclei have yielded information which helps us develop a picture of nuclear structure. But the situation is more complicated for the nucleus than for the atom. In the nucleus there are two kinds of particles, protons and neutrons, packed close together, and there are two kinds of forces – the electrostatic force and the short range strong nuclear force. This more complex situation has caused slow progress in developing a satisfactory model, and no single nuclear model has been able to explain all the nuclear phenomena.

### 11.1.1. *Some general nuclear properties*

Let us begin with a summary of what we know about the nucleus, and see where that leads us.

In Chapter 3 we observed that the binding energy per nucleon is almost constant for the stable nuclei (Fig. 3.3) and that the radius is proportional to the cube root of the mass number. We have interpreted this as reflecting fairly uniform distribution of charge and mass throughout the volume of the nucleus. Other experimental evidence supports this interpretation (Fig. 3.4). This information was used to develop the liquid drop model, which successfully explains the valley of stability (Fig. 3.1). This overall view also supports the assumption of a strong, short range nuclear force.

A more detailed consideration of Figures 3.1 and 3.3 indicates that certain mass numbers seem to be more stable, i.e. nuclei with *Z*- or *N*-values of 2, 8, 20, 28, 50, and 82 (see also Table 3.1). There is other evidence for the uniqueness of those numbers. For example, if either the probability of capturing a neutron (the neutron capture cross-section) or the energy required to release a neutron is plotted for different elements, it is found that

maxima occur at these same neutron numbers, just as maxima occur for the electron ionization energy of the elements He, Ne, Ar, Kr, etc. (i.e. at electron numbers of 2, 8, 16, 32, etc.). The nuclear *N*- or *Z*-values of 2, 8, 20, 28, 50, and 82 are called "magic numbers".

It seems logical that these magic numbers indicate some kind of regular substructure in the nucleus. Moreover, since the same magic numbers are found for the neutrons and for the protons, we would further assume that the neutrons and the protons build their substructure independently of each other, but in the same way. Another fact that must be indicative of the nuclear substructure is the stability for nuclei with even proton or even neutron numbers. Since we know that the individual nucleons have spin, we could postulate that nucleons in the nucleus must pair off with opposed spins.

### 11.1.2. *Quantized energy levels*

The nucleus would thus seem to consist of independent substructures of neutrons and protons, with each type of nucleon paired off as far as possible. Further, the nucleons obviously grouped together in the magic numbers. From the decay of radioactive nuclei we know that the total decay energy (*Q*-value) of any particular nuclide has a definite value. Moreover, γ-emission from any particular nucleus involves discrete, definite values. These facts resemble the quantized emission of electromagnetic radiation (X-ray, UV, visible light,

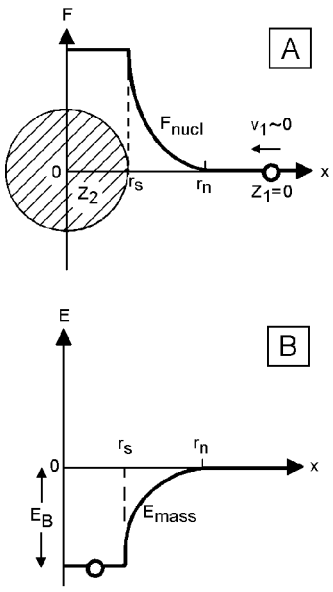


FIG. 11.1 The approach along the $x$-axis of a neutron (charge $Z_1 = 0$, velocity $v_1 \approx 0$) towards a nucleus (charge $Z_2$; Fig. A) leading to the neutron being trapped at a certain energy level, $E_B$ (Fig. B). $F_{nucl}$ is the nuclear force extending from the surface of the "solid core" at $r_s$ to the distance $r_n$. $E_B$ is the nuclear binding energy in the potential well.

etc.) from atoms. We may conclude a similar explanation for the nucleus: decay of radioactive nuclei, whether α, β, or γ, involves a transition between discrete quantized energy levels.

### 11.1.3. *The nuclear potential well*

In our development of a model of the nucleus we have so far not considered the nuclear binding energy. Let us imagine the situation wherein a neutron of low kinetic energy approaches a nucleus (Fig. 11.1). Since the neutron is uncharged it is not affected by the Coulomb field of the nucleus and approaches the nucleus with no interaction, until it is close enough to experience the strong nuclear force $F_n$, which is always attractive, i.e. $F_n$ is a positive quantity. At the point $r_n$ the neutron experiences the strong attraction to the nucleus and is absorbed. The surface of the nucleus is assumed to extend to $r_s$ since this distance represents the radius of the nucleus over which the nuclear force is constant. When the neutron is absorbed, energy is released and emitted in the form of a γ-quantum. The energy of the γ-ray can be calculated from the known masses of the reactants and product nuclides: $E_\gamma = -931.5(M_{A+1} - M_A - M_n)$.

The energy released is the (neutron) *binding energy* of the nucleus $E_B$. The total energy of the nucleus has thus decreased as is indicated in Figure 11.1(B); it is common to refer to this decrease as a *potential well*. The nucleons can be considered to occupy different levels in such a potential well. The exact shape of the well is uncertain (parabolic, square, etc.) and depends on the mathematical form assumed for the interaction between the incoming particle and the nucleus.

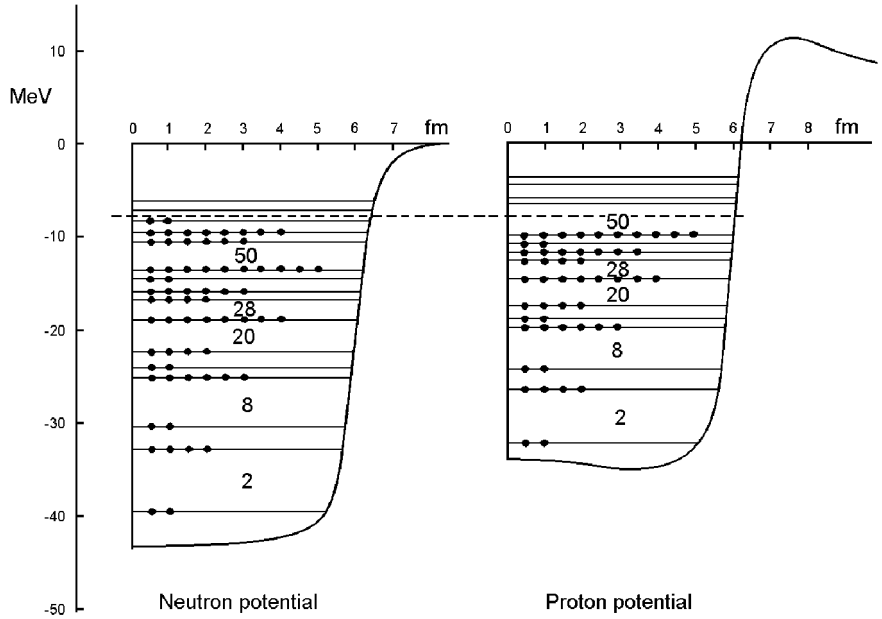


FIG. 11.2. The $^{116}$Sn neutron and proton shell structure in the potential well. (According to S. G. Nilsson.)

Protons experience the same strong, short range nuclear force interaction as they contact the nucleus. However, they also experience a long range repulsive interaction due to the Coulomb force between the positive incoming protons and the positive charge of the nucleus. This repulsion prevents the potential well from being as deep for protons as for neutrons. Figure 11.2 shows the energy levels of the protons and of the neutrons in the nucleus of $^{116}_{50}$Sn.

## 11.2. Rotational energy and angular momentum

It is an intriguing fact that nucleons in nuclei, electrons in atoms, as well as large cosmic objects such as solar systems and even galaxies, are more dominated by rotational than by linear motion, although in our daily life the latter seems to be a more common phenomenon. In rotation there is a balance between two forces: the centrifugal force of inertia, which tries to move a body away from a center point, and an attractive force (gravitational, electrostatic, etc.), which opposes the separation.

In the preceding section we assumed that the nucleus existed in some kind of a potential well. One may further assume that a nucleon moves around in this well in a way not too different from the way the electron moves around the atomic nucleus, i.e. with an oscillation between kinetic and potential energy. With some hypothesis about the shape of the nuclear potential well we can apply the *Schrödinger wave equation* to the nucleus. Without being concerned at this point with the consequences of assuming different shapes we can conclude that the solution of the wave equation allows only certain energy states. These energy states are defined by two quantum numbers: the *principal quantum number n*, which is related to the total energy of the system, and the *azimuthal* (or *radial*) *quantum number l*, which is related to the rotational movement of the nucleus.

### 11.2.1. *Rotational (mechanical) energy*

If a mass $m$ circles in an orbit of radius $r$ at a constant angular velocity $\omega$ (rad $s^{-1}$), the tangential velocity at this radius is

$$v_r = \omega r \tag{11.1}$$

The kinetic energy in linear motion is $E_{kin} = \frac{1}{2}mv^2$, and we therefore obtain for the (kinetic) rotational energy

$$E_{rot} = \frac{1}{2}m\omega^2 r^2 \tag{11.2a}$$

The angular velocity is often expressed as the frequency of rotation, $\upsilon_r = \omega/2\pi$ $s^{-1}$. Equation (11.2a) can also be written

$$E_{rot} = \frac{1}{2}I_{rot}\,\omega^2 \tag{11.2b}$$

where

$$I_{rot} = \sum m_i r_i^2 \tag{11.3}$$

is the rotational *moment of inertia*. We consider as the rotating body a system of *i* particles of masses $m_i$, each individual particle at a distance $r_i$ from the axis of rotation; then (11.2b) is valid for any rotating body. In nuclear science we primarily have to consider two kinds of rotation: the *intrinsic rotation* (or *spin*) of a body around its own axis (e.g. the rotation of the earth every 24 h), and the *orbital rotation* of an object around a central point (e.g. rotation of the earth around the sun every 365 days). Equation (11.2b) is valid for both cases, but (11.2a) only for the orbital rotation of a particle of small dimensions compared to the orbital radius, in which case $I_{rot} = mr^2$. For a spherical homogeneous spinning body (e.g. the earth's intrinsic rotation) of external radius $r_{ex}$, (11.2b) must be used, where $I_{rot} = 2mr_{ex}^2/5$.

### 11.2.2. *Angular momentum*

Like linear motion, rotation is associated with a momentum, called the *angular momentum*. For the orbital rotation the *orbital angular momentum* ($p_l$) is

$$p_l = mv_r r \tag{11.4a}$$

while for spin the spin angular momentum ($p_s$) is

$$p_s = \omega I_{rot} \tag{11.4b}$$

Angular momentum is a *vector quantity*, which means that it has always a certain orientation in space, depending on the direction of rotation. For the rotation indicated in

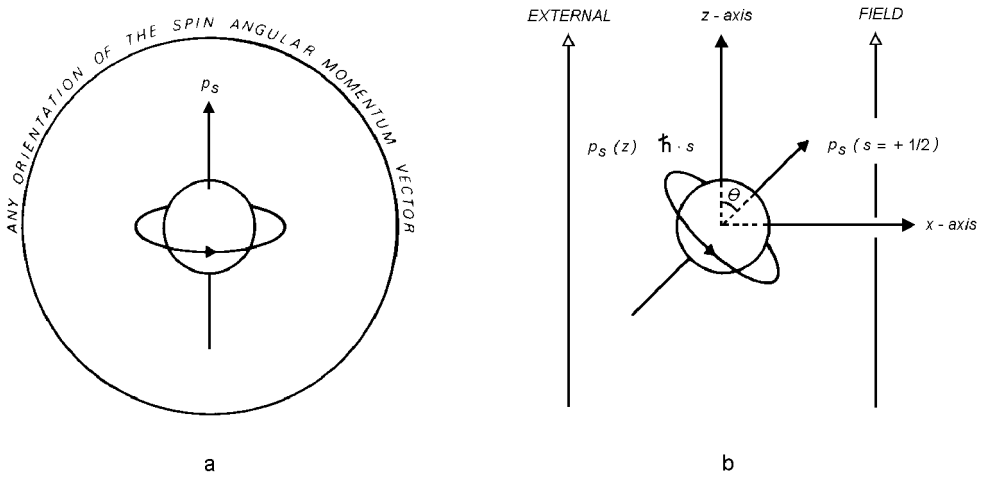


FIG. 11.3. A particle spinning in (a) field-free space and (b) in an external field along the *z*-axis.

Figure 11.3(a), the vector can only point upwards. It would not help to turn the picture upside down because the coupling between rotational direction and its vector remains the same, as students south of the equator will agree.

Quantum mechanics prescribes that the spin angular momentum of electrons, protons, and neutrons must have the magnitude

$$p_s = [s(s+1)]^{1/2} \tag{11.5}$$

here $s$ is the *spin quantum number*. For a *single* particle (electron or nucleon) the spin $s$ is always 1/2. In addition to spin, the three atomic particles can have orbital movements. Again quantum mechanics prescribes that the magnitude of the orbital angular momentum of these particles

$$p_l = [l(l+1)]^{1/2} \tag{11.6}$$

We shall refer to $l$ as the *orbital* (*angular momentum*) *quantum number*. Only certain values are permitted for $l$, related to the main quantum number $n$:

| | | |
|---|---|---|
| for electrons: | 0 | $l < n-1$ |
| for nucleons: | 0 | $l$ |

For nucleons but not for electrons $l$ may (and often does) exceed $n$.

### 11.2.3. *Coupling of spin and orbital angular moments*

A rotating charge gives rise to a *magnetic moment* $_s$. The rotating electron and proton can therefore be considered as tiny magnets. Because of the internal charge distribution of the neutron it also acts as a small magnet. In the absence of any external magnetic field these magnets point in any direction in space (Fig. 11.3(a)), but in the presence of an external field they are oriented in certain directions determined by quantum mechanical rules. This is indicated by the angle $\theta$ in Figure 11.3(b), when we have the spinning particle in the center of a coordinate system. The quantum mechanical rule is that the only values allowed for the projections of spin angular momentum $p_s(z)$ on the field axes are:

$$p_s(z) = m_s \tag{11.7}$$

For composite systems, like an electron in an atom or a nucleon in a nucleus, the (*magnetic*) *spin quantum number* $m_s$ may have two values, $+1/2$ or $-1/2$, because the spin vector has two possible orientations (up or down) with regard to the orbital angular momentum.

The orbital movement of an electron in an atom, or of a proton in the nucleus, gives rise to another magnetic moment ( $_l$) which also interacts with external fields. Again quantum mechanics prescribes how the orbital plane may be oriented in relation to such a field (Fig. 11.4(a)). The orbital angular momentum vector $p_l$ can assume only such directions that its projection on the field axes, $p_l(z)$, has the values

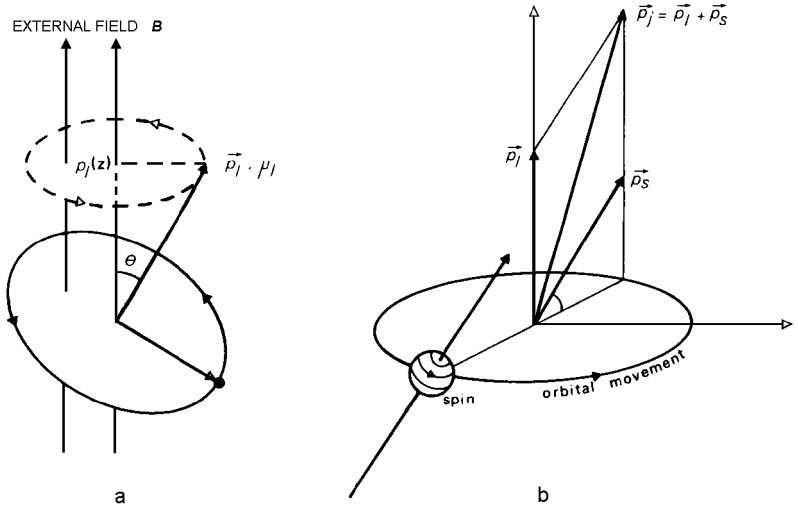


FIG. 11.4. (a) Angular momentum caused by an orbiting particle and permitted value projected on the external field axis. The vector $p_l$ precesses around the field axis as indicated by the dashed circle (ellipse in the drawing). (b) The $l$–$s$ coupling of orbital angular momentum and spin leads to a resultant angular momentum $p_j$.

$$p_l(z) = m_l \tag{11.8}$$

$m_l$ is referred to as the *magnetic orbital quantum numbers; $m_l$* can have all integer values between $-l$ and $+l$.

For a single-particle, nucleon or electron, the orbital and spin angular moments add vectorially to form a *resultant* vector (Fig. 11.4(b)),

$$p_j = p_l + p_s \tag{11.9}$$

$p_j$ will orient itself towards an external field so that only the projections

$$p_j(z) = m_j \tag{11.10}$$

are obtained on the field axes, $m_j$ is the *total magnetic angular momentum quantum number*; it can have all integer values between $-j$ and $+j$. The magnitude of $p_j$ is

$$p_j = [j(j+1)]^{1/2} \tag{11.11}$$

where

$$j = l \pm s \tag{11.12}$$

Here $j$ is the *total* (*resultant*) *quantum number of the particle*.

11.2.4. *Magnetic moments*

*a. Single particles*. Dirac showed in 1928 that the spin magnetic moment of the electron is:

$$\mu_s(\text{electron}) = \mathbf{e}/2\mathbf{m}_e = \mathbf{B}_e \tag{11.13}$$

where $\mathbf{B}_e = 9.273 \times 10^{-24}$ JT$^{-1}$ (joule per tesla). This value is referred to as one *Bohr magneton* (B.m.). For the proton one would expect the spin magnetic moment $\mu_s$ to be

$$\mathbf{B}_e\, \mathbf{m}_e/\mathbf{m}_p = \mathbf{B}_n \tag{11.14}$$

$\mathbf{B}_n$ (n for nucleon) has the value $5.051 \times 10^{-27}$ JT$^{-1}$ and is referred to as one *nuclear magneton* (n.m.). However, measurements show that

$$\mu_s(\text{proton}) = 14.1 \times 10^{-27}\ \text{JT}^{-1} = 2.793\ \text{n.m.}$$

The reason for the higher value is found in the uneven charge distribution within the proton.

Recall that the neutron also has an uneven charge distribution. This gives rise to a neutron spin magnetic moment

$$\mu_s(\text{neutron}) = -1.913\ \text{n.m.}$$

The magnetic moment $\mu_l$, caused by a charge $q$ in *circular orbit*, can be calculated from classical physics: the current caused in the orbit, $qv_r$, times the area encircled, $\pi r^2$. Therefore

$$\mu_l = qv_r\, r/2 \tag{11.15}$$

Dividing (11.15) by $p_l$ according to (11.4a), gives

$$\gamma = \mu_l/p_l = q/2m \tag{11.16a}$$

This ratio $\gamma$ is called the *gyromagnetic ratio*. If $\gamma$ and $p_l$ are known, $\mu_l$ may be calculated. Equation (11.16a) is valid for electrons ($\mathbf{e}$, $\mathbf{m}_e$), but for protons only the left part. Because of the quantization of $p_l(z)$ (11.8) the component of the orbital magnetic moment in the field direction (Fig. 11.4(a)) is also quantized:

$$\mu_l(\text{electron}) = m_l\mathbf{B}_e \tag{11.17}$$

Such a simple approach is not possible for a nucleon in a nucleus, because no nucleon moves completely independent of the other nucleons, nor is the orbital path always circular.

*b. Atoms and nuclei*. In an atom with many electrons, the spin and angular moments of the electrons couple vectorially and separately to form resultant quantum numbers (using

TABLE 11.1. *Summary of the properties of the atomic constituents (independent movements in a central potential field).*

| Line | Property | Electron | Proton | Neutron |
|---|---|---|---|---|
| 1 | Mass(u) | 0.000 5486 | 1.007 276 | 1.008 665 |
| 2 | Charge (**e** units) | −1 | +1 | −1 |
| 3 | Spin quantum number s | 1/2 | 1/2 | 1/2 |
| 4 | Spin dipole moment | $\mu_e = 1$ B.m. | $\mu_p = 2.793$ n.m. | $\mu_n = -1.913$ n.m. |
| 5 | Orbital quantum number | $0 \; l \; n-1$ | $0 \; l$ | |
| 6 | Permitted orbital field projections | $-l \ldots +l$ | $-l \ldots +l$ | |
| 7 | Total angular quantum number | $(j = l \pm s)$ | $j = l \pm s$ | |
| 8 | Total angular momentum | $(p_j = \sqrt{(j(j+1))})$ | $p_j = \sqrt{(j(j+1))}$ | |
| 9 | Particle symbolism | $nl^i$ | $nl_j$ | |

*Notes*

2. The electron unit charge: $\mathbf{e} = 1.602 \times 10^{-19}$ C.

3. The spin angular momentum has the magnitude $p = \sqrt{(s(s+1))}$, with the permitted projections on an external field axis: $\pm s$ (for e, p, and n = ½).

7. $l$ and $s$ couple only in the one-electron system; see §11.2.4.

8. Permitted projections on an external field axis: $m_j$, where $-j \; m_j \; j$.

9. $n$ is the principal quantum number, $l$ the azimuthal (orbital, radial) quantum number, $i$ is the number of electrons in the particular $n,l$ state, and $j$ is the total angular momentum quantum number. For $l = 0$, 1, 2, etc., the symbols s, p, d, f, g, etc., are used.

TABLE 11.2. *Summary of atomic and nuclear properties associated with particle interactions (q.n. = quantum number).*

| Line | Property | Electron-electron interaction | Nucleon-nucleon interaction |
|---|---|---|---|
| 10 | Spin-spin ($s$-$s$) coupling, q.n. | $S = \Sigma s_i$ (strong) | (For each nucleon $j = l \pm s$ |
| 11 | Total spin magnetic moment | $\mu_s = 2(S(S+1))^{½}$B.m. | and $I = \Sigma j_i$ ) |
| 12 | Orbit-orbit ($l$-$l$) coupling, q.n. | $L = \Sigma l_i$ (strong) | (For ee nuclei: groundstate $l = 0$ |
| 13 | Total orbital magnetic moment | $\mu_L = 2(L(L+1))^{½}$B.m. | For eo, oe nuclei: groundstate $l = j$ |
| 14 | Spin-orbit coupling, q.n. | $J = S + L$ (weak) | \For oo nuclei: groundstate varies |
| 15 | Resulting angular momentum | $p_J = (J(J+1))^{½}$B.m. | $p_I = (I(I+1))^{½}$n.m. |
| 16 | Resulting magnetic moment | $\mu_J = g_J(J(J+1))^{½}$B.m. | $\mu_I = g_I(I(I+1))^{½}$n.m. |
| 17 | Transition selection rules | $\Delta L \pm 1$, $\Delta J = 0$ or $\pm 1$ | $\Delta_I$ = integer, $\Delta_j > 0$ |
| 18 | Multipole moment | Electric dipole | Electric or magnetic multipole |
| | | Electron-nucleon interactions | |
| 19 | Grand atomic angular mom., q.n. | $F = J + I = S + L + I$ | |
| 20 | Grand atomic angular mom. | $p_F = (F(F+1))^{½}$; field projections 0,…, $F$ | |
| 21 | External field: none | Hyperfine spectrum (hfs): $J$ levels split due to nuclear spin $I$ | |
| 22 | External field: weak ( $10^{-2}$ T) | Hfs $F$-levels split into $2F+1$ levels (Zeeman effect) | |
| 23 | External field: average ( 10 T) | Electron-nucleon q.n. decouple, producing $(2J+1)(2I+1)$ levels | |
| 24 | External field: very strong | Electron spin-orbit decouple, producing separate $S$- and $L$-levels | |

conventional symbolism)

$$S = \sum s_i \tag{11.18a}$$

$$L = \sum l_i \tag{11.18b}$$

which couple to form the total angular momentum (or internal) quantum number of the atom

$$J = L + S \tag{11.18c}$$

(see Table 11.2). Equations (11.18) are referred to as *Russell-Saunders coupling*. For the atom as a whole, the magnetic moment is

$$(\text{atom}) = g_j \, \mathbf{e} \, p_j / 2 \, \mathbf{m}_\text{e} = g_j \, \mathbf{B}_\text{e} \, m_j \tag{11.19}$$

where $g_j$ is the Landé factor and $+J \quad m_j \quad -J$. The Landé factor accounts for the effect of mutual screening of the electrons.

The *nuclear magnetic moment* depends on the spin and angular moments of the neutrons and protons. For the nucleus it is given by

$$(\text{nucleus}) = g_I \, \mathbf{e} \, p_I / 2 \, \mathbf{m}_\text{p} \tag{11.20}$$

where $g_I$ is the nuclear $g$-factor and $p_I$, the magnitude of the nuclear spin angular moment. Because this moment can have only the projections $m_I$ on the axes of a magnetic field where $m_I$ is the nuclear magnetic angular momentum quantum number ( $-I \quad m_I \quad I$), we may write this equation

$$(\text{nucleus}) = g_I \, (\mathbf{e} \quad / 2 \, m_p) m_I = g_I \, \mathbf{B}_\text{n} \, m_I \tag{11.21}$$

$I$ is the *total nuclear spin*. We shall see in the next section how $I$ can be determined.

In Table 11.1 we have summarized the most important properties of the atomic constituents, and in Table 11.2 their modes of interaction. In Table 11.3 some spin and magnetic moments are given for stable and radioactive nuclei.

### 11.2.5. *Precession*

Before going into the details of nuclear structure, there is one more property of the nucleon which must be considered. Both types of angular momenta, $p_s$ and $p_l$, as well as their corresponding magnetic moments, are vector quantities. Quantum mechanics forbids $p$ (and consequently ) to be exactly parallel with an external field. At the same time the external field tries to pull the vector so that the plane of rotation becomes perpendicular to the field lines. The potential magnetic energy is

$$E_\text{magn} = B \quad = B \quad \cos \theta \tag{11.22}$$

TABLE 11.3. *Spin I, parity* (+ *even*, − *odd*), *nuclear magnetic moment* (μ n.m.) *and quadrupole moment Q* ($10^{-28}$ $m^2$) *for some nuclides* $^{A}X$

| Stable nuclides | | | | Radioactive nuclides | | | | |
|---|---|---|---|---|---|---|---|---|
| $^{A}X$ | $I$ (±) | $\mu_I$ | $Q$ | $^{A}X$ | $I$ (±) | $\mu_I$ | $Q$ | $t_{½}$ |
| $^{1}H$ | 1/2 + | +2.793 | | $^{3}H$ | 1/2 + | +2.979 | | 12.33 y |
| $^{2}H$ | 1 + | +0.857 | +0.003 | $^{14}C$ | 0 + | | | 5730 y |
| $^{10}B$ | 3 + | +1.801 | +0.085 | $^{24}Na$ | 4 + | +1.690 | | 14.959 h |
| $^{11}B$ | 3/2 − | +2.689 | +0.041 | $^{32}P$ | 1 + | −0.252 | | 14.262 d |
| $^{12}C$ | 0 + | | | $^{36}Cl$ | 2 + | +1.285 | −0.018 | $3.01 \times 10^{5}$ y |
| $^{13}C$ | 1/2 − | +0.702 | | $^{45}Ca$ | 7/2 − | −1.327 | +0.046 | 163.8 d |
| $^{14}N$ | 1 + | +0.404 | +0.019 | $^{55}Fe$ | 3/2 − | | | 2.73 y |
| $^{16}O$ | 0 + | | | $^{60}Co$ | 5 + | +3.799 | +0.44 | 5.271 y |
| $^{17}O$ | 5/2 + | −1.894 | −0.026 | $^{64}Cu$ | 1 + | −0.217 | | 12.70 h |
| $^{19}F$ | 1/2 + | +2.629 | | $^{95}Zr$ | 5/2 + | | | 64.02 d |
| $^{23}Na$ | 3/2 + | +2.218 | +0.101 | $^{131}I$ | 7/2 + | +2.742 | −0.40 | 8.0207 d |
| $^{31}P$ | 1/2 + | +1.132 | | $^{137}Cs$ | 7/2 + | +2.841 | +0.051 | 30.0 y |
| $^{33}S$ | 3/2 + | +0.644 | −0.076 | $^{140}La$ | 3 − | +0.730 | +0.094 | 1.678 d |
| $^{39}K$ | 3/2 + | +0.391 | +0.049 | $^{198}Au$ | 2 − | +0.593 | +0.68 | 2.6952 d |
| $^{59}Co$ | 7/2 − | +4.627 | +0.404 | $^{232}Th$ | 0 + | | | $1.405 \times 10^{10}$ y (α) |
| $^{87}Sr$ | 9/2 + | −1.094 | +0.335 | $^{235}U$ | 7/2 − | −0.38 | +4.55 | $7.038 \times 10^{8}$ y (α) |
| $^{141}Pr$ | 5/2 + | +4.275 | −0.059 | $^{238}U$ | 0 + | | 13.9 | $4.468 \times 10^{9}$ y (α) |
| $^{197}Au$ | 3/2 + | +0.146 | +0.547 | $^{239}Pu$ | 1/2 + | +0.203 | | $2.411 \times 10^{4}$ y (α) |

(see Figs. 11.3 and 11.4) where $B$ is the magnetic field strength. However, because of the inertia of the particle this does not occur until the particle has moved somewhat along its orbit, with the consequence that the vector starts to rotate around the field axes as shown in Figure 11.4(a). The angular momentum vector therefore precesses around the field axes, like a gyroscope. We may rewrite (11.16a) as

$$\gamma = /p_{\text{rot}} \tag{11.16b}$$

This form makes it more obvious why γ is referred to as the gyromagnetic ratio. Equation (11.16b) is valid both for angular momentum and spin, but of course the value is different for electrons and protons. The angular velocity $\omega_\gamma$ of the precession is found to be

$$\omega_\gamma = B/p_{\text{rot}} \tag{11.23}$$

By replacing angular velocity with frequency ($\omega = 2\pi\upsilon$)

$$\upsilon_\gamma = \gamma B /2\pi p_{\text{rot}} \tag{11.24a}$$

or

$$\upsilon_\gamma = \gamma B/2\pi \tag{11.24b}$$

where $\upsilon_\gamma$ is the Larmor precession frequency.

## 11.3. The single-particle shell model

### 11.3.1. *Quantum number rules*

Let us assume that a nucleon moves around freely in the nuclear potential well, which is spherically symmetric, and that the energy of the nucleon varies between potential and kinetic like a harmonic oscillator, i.e. the potential walls (see Figs. 11.1 and 11.2) are parabolic. For these conditions the solution of the Schrödinger equation yields:

$$E(\text{nucleon}) = (2U_0/mr^2)^{1/2}\,[2(n-1)+l] \tag{11.25}$$

where $U_0$ is the potential at radius $r = 0$ and $m$ is the nucleon mass. We have defined $n$ and $l$ previously. The square root, which has the dimension $s^{-1}$, is sometimes referred to as the oscillator frequency ($\omega$ in Table 11.6). The following rules are valid for nucleons in the nuclear potential well:

(a) $l$ can have all positive integer values beginning with 0, independent of $n$;

(b) the energy of the $l$ state increases with increasing $n$ as given by (11.25);

(c) the nucleons enter the level with the lowest total energy according to (11.25) independent of whether $n$ or $l$ is the larger;

(d) there are independent sets of levels for protons and for neutrons;

(e) the Pauli principle is valid, i.e. the system cannot contain two particles with all quantum numbers being the same;

(f) the spin quantum numbers must be taken into account (not included in (11.25)).

TABLE 11.4. *Energy levels derived on basis of permitted values for the azimuthal quantum number l and spin quantum number s*

| $l$ | State | Possible quantum values | Number of states (including spin) | Accumulated nucleon number |
|---|---|---|---|---|
| 0 | s | 0 | 1 x 2 = 2 | 2 |
| 1 | p | $-1, 0, +1$ | 3 x 2 = 6 | 8 |
| 2 | d | $-2, -1, 0, +1, +2$ | 5 x 2 = 10 | 18 |
| 3 | f | $-3, -2, -1, 0, +1, +2, +3$ | 7 x 2 = 14 | 32 |
| 4 | g | $-4, -3, -2, -1, 0, +1, +2, +3, +4$ | 9 x 2 = 18 | 50 |
| $l$ | - | $-l, \ldots, +l$ | $2(2l+1)$ | - |

TABLE 11.5. *Energy levels according to equation* (11.25)

| Levels | Number of nucleons | Accumulated nucleons |
|---|---|---|
| 1s | 2 | 2 |
| 1p | 6 | 8 |
| 1d and 2s | 10 + 2 | 20 |
| 1f and 2p | 14 + 6 | 40 |
| 1g, 2d, and 3s | 18 + 10 + 2 | 70 |
| 1h, 2f, and 3p | 22 + 14 + 6 | 112 |
| ... | ... | ... |

Following these rules, the nucleons vary greatly in energy and orbital motion. However these rules do not exclude the existence of two nucleons with the same energy (so-called degenerate states), provided the quantum numbers differ.

### 11.3.2. *Nuclei without nucleon spin-orbit coupling*

If we calculate the sequence of energy levels on the assumption that $n$ is constant, we obtain the pattern in Table 11.4. This is the sequence of electronic states in atoms but it does not agree with the observed magic numbers 2, 8, 20, 28, 50, etc., for nuclei.

Applying the rules of the previous section a new set of nucleon numbers is obtained: 2, 8, 20, 40, 70, etc. (Table 11.5, and left column Table 11.6). This level scheme allows a large amount of degeneracy. For example, for $n = 1$ and $l = 3$ (1f-state) we find from (11.25) that $[2(n-1)+l] = 3$, which value is obtained also for $n = 2$ and $l = 1$ (2p-state). Since the f-state can have 14 and the p-state 6 nucleons, the degenerate level of both states can contain 20 nucleons. However, the numbers still do not correspond to the experimental magic numbers.

A further refinement is possible if we assume that the nuclear potential well has straight walls, i.e. the potential energy $U(r)$ is $-U_o$ at $r < r_n$ while it is infinite at $r \geq r_n$, where $r_n$ is the nuclear radius. This assumption, when introduced (see Fig. 11.2 and figure in Table 11.6) in the Schrödinger-equation, leads to a splitting of the degenerate levels, so that the lowest energy is obtained for the state with lowest main quantum number $n$. For our example of the 1f and 2p-states the 1f orbitals are lower in energy than the 2p. This refinement yields the middle row of levels in Table 11.6 but still does not lead to the correct magic numbers.

### 11.3.3. *Nuclear level scheme with nucleon spin-orbit coupling*

In multielectron atoms, the Russell-Saunders coupling is present in light atoms. However, in the heaviest atoms of many electrons and in highly charged nuclei, the *j-j* (spin-orbit) coupling better describes the systems. Haxel, Jensen, Suess, and Goeppert-Mayer in 1949 suggested that the nucleons always experience a strong spin-orbit coupling according to (11.12)

TABLE 11.6. *Nuclear energy levels obtained for the single-particle model by solving the Schrödinger-equation (a) for a harmonic oscillator and rounded square-well potentials (b) without and (c) with spin–orbit coupling. The $n\hbar\omega$ figures to the left are energies for model a, according to eqn.*(11.25). *Numbers in* ( ) *indicate orbital capacities and those in* [ ] *give cumulative capacity up to the given line.* (From Gordon and Coryell)

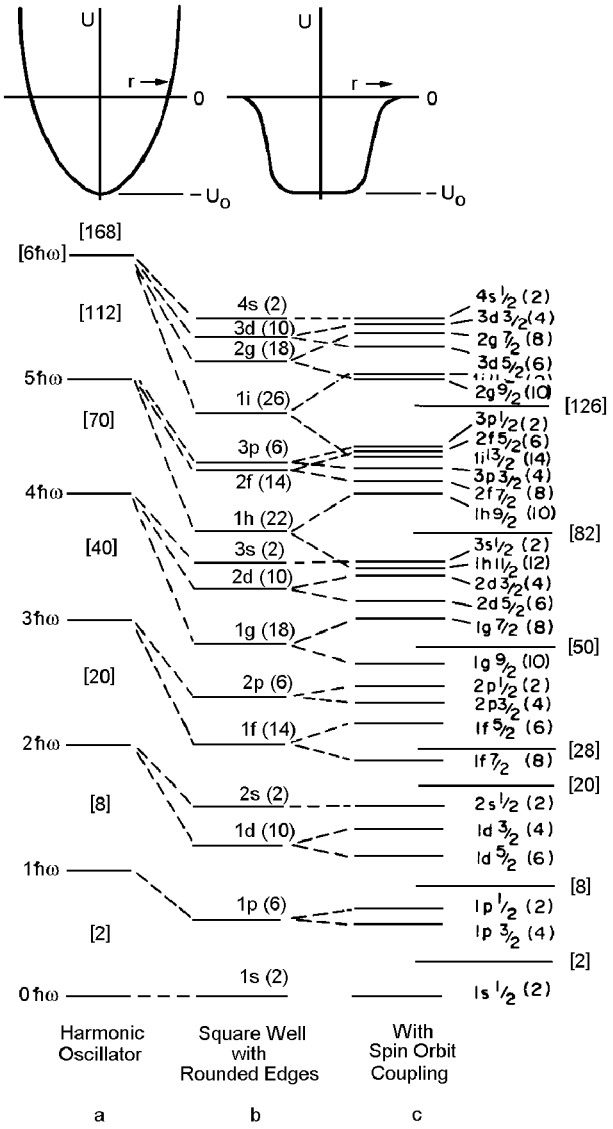

$$j = l \pm s \tag{11.12}$$

and that the total spin of the nucleus $I$ is the sum of the nucleon spins

$$I = \sum j \tag{11.26}$$

In this way, all $I$ levels are split into two levels with quantum values $l + 1/2$ and $l - 1/2$, of which the former has the lowest energy value (the opposite of the electron case). This yields the row of levels on the right in Table 11.6. Because of the energy splitting the new levels group together so they fit exactly with the experimental magic numbers.

As an example, consider the level designation $1i_{11/2}$. This has the following interpretation: the principal quantum number is 1; i indicates that the orbital quantum number $l$ is 6; the angular momentum quantum number $j$ is 11/2 ($j = l - 1/2$). The number of permitted nucleons in each level is $2j + 1$, thus 12 for $j = 11/2$.

The magic numbers correspond to sets of energy levels of similar energy just as in the atom the K, L, M, etc., shells represent orbitals of similar energy. The N-electronic shell contains the 4s, 3d, 4p sets of orbitals while the 4th nuclear "shell" contains the $1f_{5/2}$, $2p_{3/2}$, $2p_{1/2}$, and $1g_{9/2}$ sets of orbitals. Remember that there are separate sets of orbitals for protons and for neutrons.

### 11.3.4. *The nuclear spin*

The nuclear spin $I$ is obtained from (11.12) and (11.26). Since $j$ is always a half-integer, nuclides with odd number of nucleons (odd $A$) must have odd spin values (odd $I$), while those with even $A$ must have even $I$. The nucleons always pair, so that even numbers of protons produce no net spin. The same is true for even numbers of neutrons. For nuclei of even numbers for both $N$ and $Z$, the total nuclear spin $I$ is always equal to zero. Some ground state nuclear spins are given in Table 11.3.

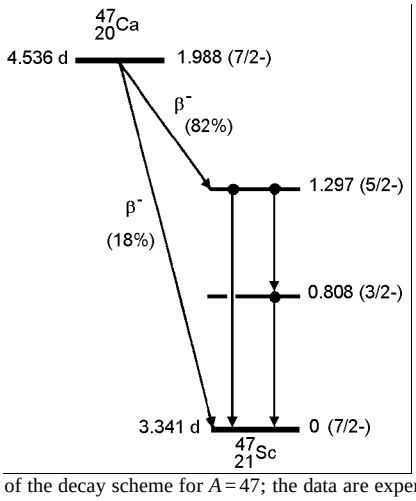


FIG. 11.5. Part of the decay scheme for $A = 47$; the data are experimental values.

For odd $A$ the nuclear spin is wholly determined by the single unpaired nucleon (single particle model). Let us take the nucleus $^{13}_{6}C$ as an example. It contains 6 protons and 7 neutrons. From Table 11.6 we conclude that there are 2 protons in the $1s_{1/2}$ level and 4 protons in the $1p_{3/2}$ level. A similar result is obtained for the first 6 neutrons but the 7th neutron must enter the $1p_{1/2}$ level. The value of $I$ for $^{13}C$ is thus 1/2. Another example is $^{51}_{23}V$, which has 23 protons and 28 neutrons. Since $N = 28$, the neutrons do not contribute to $I$. From Table 11.6 we see that we can accommodate 20 protons in the orbitals $1s^2$, $1p^6$, $1d^{10}$ ,$2s^2$. The next 3 protons must go into the $1f_{7/2}$ level ($1f^3_{7/2}$), where, however, 2 of them are paired. Therefore, the single unpaired proton has $j = 7/2$, leading us to predict $I = 7/2$, which also is the measured nuclear spin value.

When a nucleus is excited, either through interaction with other particles or in a decay process, for nuclei with $N$ or $Z$ values near magic numbers the paired nucleons seem not to be perturbed by the excitation (if it is not too large). As a result, we can associate the excitation with any unpaired nucleons. Let us choose the decay of $^{47}Ca$ to $^{47}Sc$ (see Fig. 11.5). $^{47}Ca$ has 27 neutrons and in the ground state the last 7 neutrons must occupy the $1f_{7/2}$ level. The ground state of (the unstable) $^{47}Sc$ has 21 protons, the unpaired proton can only be accommodated in the $1f_{7/2}$ level. Thus both of the ground states have $I = 7/2$. The next higher energy states for $^{47}Sc$ involve the levels $1f_{5/2}$ and $2p_{3/2}$. In the Figure it is seen that these levels are observed although their order is reversed from that in Table 11.6. This reflects some limitation of the single-particle model, and is explained in §11.5.

For odd-odd nuclei the nuclear spin is given by

$$I(\text{odd-odd}) = j_p + j_n = (l_p \pm 1/2) + (l_n \pm 1/2) \tag{11.27a}$$

According to the rules formulated by Brennan and Bernstein (useful in the range $20 < A < 120$ for ground states and low-lying longlived isomeric states), if the odd particles are both particles (or both holes) in their respective unfilled subshells then

$$\text{if } j_p + j_n + l_p + l_n \text{ is even,} \qquad \text{then } I = j_p - j_n \tag{11.27b}$$

$$\text{if } j_p + j_n + l_p + l_n \text{ is odd,} \qquad \text{then } I = j_p \pm j_n$$

$$\text{but if we have both particles and holes,} \qquad \text{then } I = j_p + j_n - 1$$

The use of these rules can be illustrated by the case of $^{64}_{29}Cu$ which has its odd proton in the $1f_{5/2}$ orbital and its odd neutron in the $2p_{3/2}$ orbital. Thus for the proton, $j = 5/2$, $l = 3$; for the neutron, $j = 3/2$, $l = 1$. Because $j_p + j_n + l_p + l_n$ is even, we use $I = 5/2 - 3/2 = 1$, which is the observed spin value. The lightest nuclei are exceptions to this rule since they often exhibit LS coupling according to (11.18). $^{10}B$ is an example; it has 5 protons and 5 neutrons, the fifth nucleon being in the $1p_{3/2}$ state. Thus $I = j_1 + j_2 = 3$, which is observed.

We mentioned in §11.2.4 that theoretical calculations of the nuclear magnetic moment, (11.21), are usually not satisfactory. The value of (nucleus) can have a number of values depending on $m_I$, with a maximum value of $I$.

The parity[1] of the nucleus follows the rules: (i) when both particles are in states either of even parity or of odd parity, they combine to a system of even parity. (ii) one particle in a state of even parity and one in a state of odd parity combine to a system of odd parity.

## 11.4. Deformed nuclei

### 11.4.1. *Deformation index*

Both the liquid-drop model and the single-particle model assume that the mass and charge of the nucleus are spherically symmetric. This is true only for nuclei close to the magic numbers; other nuclei have distorted shapes. The most common assumption about the distortion of the nuclide shape is that it is ellipsoidal, i.e. a cross-section of the nucleus is an ellipse. Figure 11.6 shows the oblate (flying-saucer-like) and prolate (egg-shaped) ellipsoidally distorted nuclei; the prolate shape is the more common. Deviation from the spherical shape is given by

$$\beta = 2(a-c)/(a+c) \tag{11.28}$$

where $a$ and $c$ are the elliptical axes as shown on in Figure 11.6c. For prolate shape $\beta > 0$, and for oblate shape $\beta < 0$. The maximum deformation observed is about $\beta = \pm 0.6$.

The deformation is related to the nuclear shell structure. Nuclei with magic numbers are spherical and have sharp boundary surfaces (they are "hard"). As the values of $N$ and $Z$ depart from the magic numbers the nucleus increases its deformation.

### 11.4.2. *Electric multipoles*

In a spherical nucleus we assume the charge distribution to be spherical and the nucleus acts as a monopole. In the deformed nuclei, the nuclear charge has a non-spherical distribution. The potential at a point $\bar{x},\bar{y},\bar{z}$ (Fig. 11.6) will be found to vary depending on the charge distribution and mode of rotation of the nucleus. The nuclear charge may be distributed to form a dipole, a quadrupole, etc. Nuclei are therefore divided into different classes depending on their electrical moments: monopoles, dipoles, quadrupoles, octupoles etc.

It has been found that nuclei with spin $I = 0$ have no multipole moment. According to theory, nuclei with $I = 1/2$ can have a dipole moment, but this has not yet been shown experimentally. Nuclei with $I = 1$ have quadrupole moments; they are fairly common. The quadrupole moment $Q$ can be calculated for spheroidal (i.e. deformation not too far from a sphere) nuclei in terms of the electron charge, **e**, by

$$Q = (2/5)\, Z\, (a^2 - c^2) \tag{11.29a}$$

[1] Parity is the behavior of wave functions when all coordinate signs are reversed. Even parity — no effect, else odd parity.

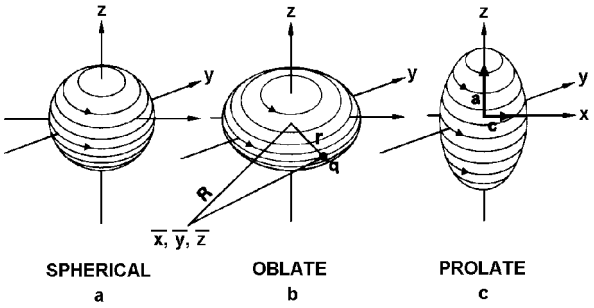


FIG. 11.6. Three nuclidic shapes: (a) spherical nucleus, (b) oblate (extended at the equator), and (c) prolate (extended at the poles).

$Q$ is usually referred to as the internal quadrupole moment, i.e. the expected value for a rotation around the $z$-axis. However, quantum mechanics makes this impossible and gives for the maximum observable quadrupole moment

$$Q_{\text{obs}} = Q(I-1/2)/(I+1) \tag{11.29b}$$

Thus $Q_{\text{obs}} = 0$ for $I \quad 1/2$. $Q_{\text{obs}}$ is usually given in area ($m^2$). Most commonly $10^{-28} m^2$ is used as unit and referred to as one barn, $Q_{\text{obs}}$ is $> 0$ for the more common prolate shape, and $< 0$ for oblate. Some measured values are given in Table 11.3.

The rotation of nuclei with electric multipoles gives rise to formation of magnetic multipoles. Nuclei can therefore also be divided according to the magnetic moments in the same way as according to their electrical moments.

### 11.4.3. *The collective nuclear model*

In 1953 A. Bohr and Mottelsen suggested that the nucleus be regarded as a highly compressed liquid, undergoing quantized rotations and vibrations. Four discrete collective motions can be visualized. In Figure 11.6 we can imagine that the nucleus rotates around the $y$-axis as well as around the $z$-axis. In addition it may oscillate between prolate to oblate forms (so-called *irrotation*) as well as *vibrate*, for example, along the $x$-axis. Each mode of such collective nuclear movement has its own quantized energy. In addition, the movements may be coupled (cf. coupling of vibration and rotation in a molecule).

The model allows the calculation of rotational and vibrational levels as shown in Figure 11.7. If a $^{238}U$ nucleus is excited above its ground state through interaction with a high energy heavy ion (coulomb excitation), we have to distinguish between three types of excitation: (a) nuclear excitation, in which the quantum number $j$ is changed to raise the nucleus to a higher energy level (according to Table 11.6); (b) vibrational excitation, in which case $j$ is unchanged, but the nucleus is raised to a higher vibrational level, characterized by a particular vibrational quantum number (indicated in the figure); (c) rotational excitation, also characterized by a particular rotational quantum number. The Figure shows that the rotational levels are more closely spaced and thus transitions between

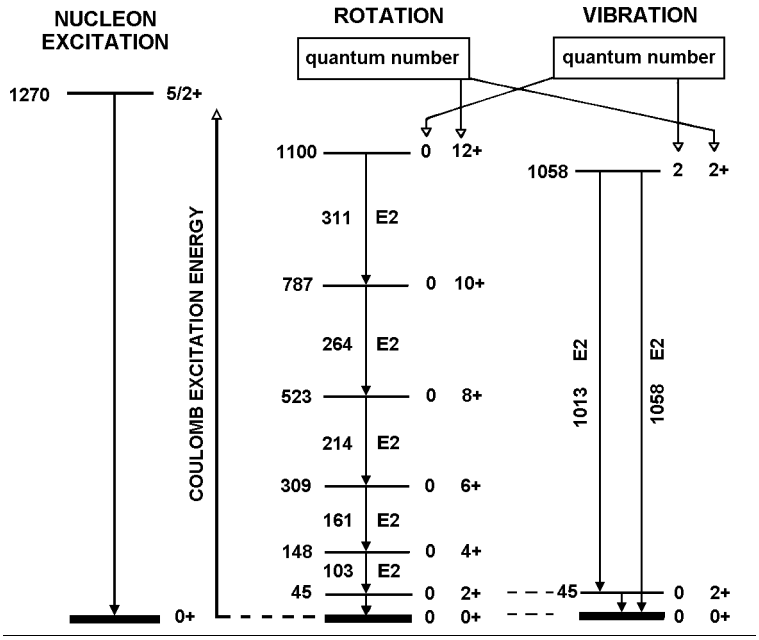


rotational levels involve lower energies than de-excitation from excited nuclear or vibrational states.

In case of even-even nuclei, the rotational energy levels can be often calculated from the simple expression

$$E_{\text{rot}} = (\ ^2/2I_{\text{rot}})n_{\text{r}}(n_{\text{r}}+1) \tag{11.30}$$

where $I_{\text{rot}}$ is the moment of inertia and $n_{\text{r}}$ the rotational quantum number; this equation is identical to (2.29). The validity of this equation depends on whether the different modes of motion can be treated independently or not, which they can for strongly deformed nuclei like $^{238}$U.

## 11.5. The unified model of deformed nuclei

The collective model gives a good description for even-even nuclei but cannot account for some of the discrepancy between observed spins and the spin values expected from the single-particle shell model. The latter was developed on the assumption of a nucleon moving freely in a symmetrical potential well, a situation which is valid only for nuclei near closed shells. The angular momentum of an odd-*A* deformed nucleus is due both to the rotational angular momentum of the deformed core and to the angular momentum of the odd nucleon. Consequently the energy levels for such a nucleus are different from those of the symmetric shell model.

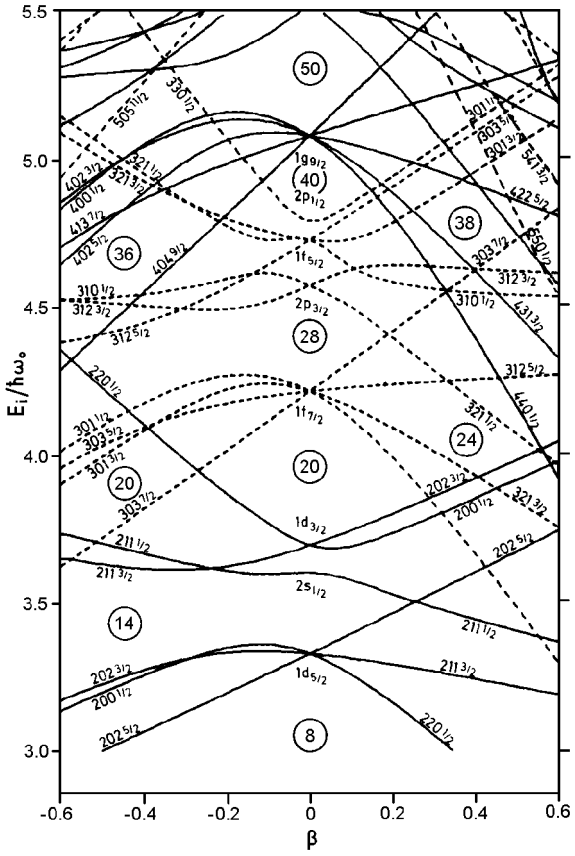


FIG. 11.8. Nilsson diagram of single-particle energy levels for deformed nuclei. The energy scale is in units of $\hbar\omega_0$ ($\hbar\omega_0$ is approximately $41A^{-1/3}$ MeV). The figures along the center give the neutron or proton numbers and $l$–$j$ values for the single nucleon. The figure combinations at the end of the lines are approximate quantum numbers; the first figure is the principal quantum number $n$. Fulldrawn lines are for even parity, broken lines for odd. (From Larsson, Leander, Ragnarsson and Alenius.)

This situation was taken into account by S. G. Nilsson, who calculated energy levels for odd nuclei as a function of the nuclear deformation β. Figure 11.8 shows how the energies of the Nilsson levels vary with the deformation β of the potential well. Each shell model level of angular momentum $j$ splits into $j + 1/2$ levels (called *Nilsson levels* or *states*). Each level may contain up to two nucleons and form the ground state of a rotational band. In addition the undeformed levels ($\beta = 0$) appear in somewhat different order than for the symmetric shell model (Table 11.6). This leads to a reversal in order for some of the levels, e.g. $1f_{5/2}$ and $2p_{3/2}$ (this explains the observed level order for $^{47}$Sc, Fig. 11.5). The Nilsson levels are quite different in all characteristics from the shell model states, and their prediction of energies, angular momenta, quantum numbers, and other properties agrees better with experimental data for deformed nuclei than those of any other model.

As an example we may choose $^{23}_{11}$Na, which has a quadrupole moment of 0.101 barn. Assuming the nuclear radius to be $1.1\ A^{1/3} = (a+c)/2$ (fm) we can use (11.28) and (11.29a) to calculate a deformation index $\beta = 0.12$. (The value 1.1 for the constant $r_o$ in (3.7) gives better agreement in nuclei where the inertia of the nucleus is involved.) From Figure 11.8 the 11th proton must enter the 3/2 level rather than the $1d_{5/2}$ level as the symmetric shell model indicates in Table 11.6. The experimental spin of 3/2 confirms the Nilsson prediction. Similarly, for the deformed $^{19}_{9}$F and $^{19}_{10}$Ne, we expect from Table 11.8 the odd nucleon to give spin of 1/2 and not 5/2, as would be obtained from Table 11.6. Again, experiment agrees with the prediction of 1/2.

## 11.6. Interaction between the nuclear spin and the electron structure

We have already seen how the spin and orbital angular momentum of the electrons and of the nucleus produce magnetic fields that interact with each other. The field produced by the electrons is much larger than that of the nucleus, and consequently the nuclear spin is oriented in relation to the field produced by the electron shell. By contrast the effects of the nuclear spin on the electron structure is so small that it usually neglected. Nuclear physics has provided us with instruments of such extreme sophistication and resolution that there are many ways of measuring with great accuracy the interaction between the nucleus and the electrons. The result has been new research tools of utmost importance, most prominent being the *nuclear magnetic resonance* (nmr) techniques. The separate disciplines of chemistry, atomic physics, nuclear physics, and solid state physics approach each other closely in such techniques, and an understanding of the theory and experimental methods requires knowledge of all these subjects.

In this section only a few important aspects of the interaction between nuclear spin and electronic structure are reviewed. The methods described are usually not considered to fall within the framework of nuclear chemistry, but in all scientific fields it is important to be able to reach the border and look at developments and techniques used on the other side. Such information is often the seed to further scientific development.

### 11.6.1. *Hyperfine spectra*

In §11.3.4 we mentioned that the electrons in the atomic shell have Russell-Saunders coupling (11.18), $J = L + S$, where $J$ is referred to as the *internal quantum number*. The magnetic field created by the electrons interacts with that caused by the nuclear spin to yield the grand atomic angular momentum vector

$$F = J + I \tag{11.31a}$$

The magnitude of this momentum is

$$p_F = [F(F+1)]^{½}, \tag{11.31b}$$

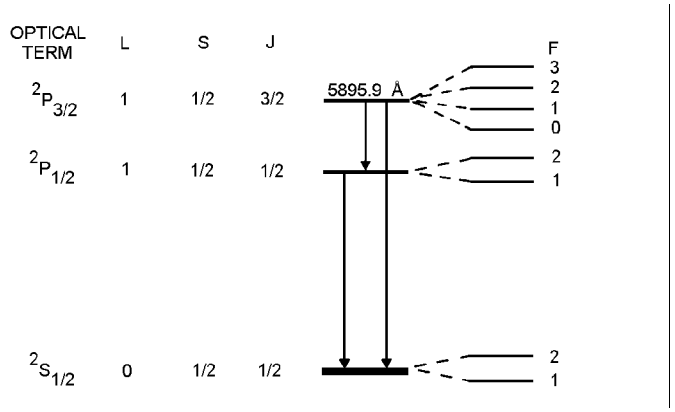


FIG. 11.9. The development of hyperfine lines in an optical spectrum of sodium due to the nuclear spin $I$, which enters through $F = J + I$.

but only projections $p_F(z) = 0, \ldots F$ are permitted on an external (to the atom) field axis. This leads to a large number of possible energy levels, although they are limited by certain selection rules.

The nuclear spin can orient itself in relation to $J$ in

$$2I + 1 \text{ directions if } I \quad J$$
$$2J + 1 \text{ directions if } J \quad I$$

Consider $^{23}$Na as an example (Fig. 11.9);[1] it has a nuclear spin $I = 3/2$. The yellow sodium line of 589.6 nm is caused by de-excitation of its electronically excited p state to the ground state $2s_{1/2}$.

The difference between the two p-states is very small, only 0.0022 eV (or about 0.6 nm), and can only be observed with high resolution (*fine spectra*). To each of these three levels the nuclear spin $I$ has to be added, yielding the quantum number $F$ according to (11.31). It is easy to determine that the level number rule holds, e.g. for $I = J$ we must have $2I + 1 = 4$ possible levels. These levels can be observed in optical spectrometers only at extremely high resolution (*hyperfine spectrum*, hfs). The energy separation between the hfs lines depends on the nuclear magnetic dipole $\quad_I$, the spin value $I$, and the strength of the magnetic field produced at the nucleus, as discussed in §11.2.4 (see also §11.6.3). The energy separation is very small, on the order of $10^{-5}$ eV, corresponding to a wavelength difference of about 1/1000 of a nm. Even if there is great uncertainty in the energy determination of the levels, simply counting the number of hyperfine lines for a certain electronic $J$-level gives the value of the nuclear spin, because $-I \quad m_I \quad I$ (number of $m_I$ values $= 2I + 1$ ).

At very high resolutions it may be possible to determine $\quad_I$ from hfs, and from this to calculate $I$. The hyperfine splitting and shifting of optical lines have yielded important information not only about nuclear spins and magnetic moments, but also about the electric charge distribution and radius of the nucleus.

[1]The letters $S$ and $P$ stand for $L = 0$ ($\Sigma l_j = 0$) and 1, respectively. The superscript 2 refers to the number of possible $S$-values; thus $2S + 1 = 2$, i.e. $S = \Sigma s_i = 2$. The subscript gives the $J$-value.

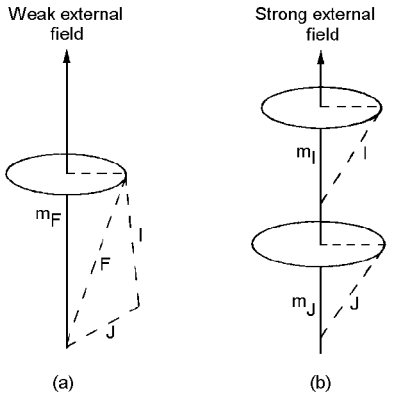


FIG. 11.10. (a) Coupling of electronic and nuclear angular moments $J$ and $I$ in a very weak magnetic field. Their sum $F$ forms the quantum number $m_F$ along the direction of the magnetic field, the maximum magnitude of which is $p_F(z) = \hbar F$. In a strong magnetic field the electronic and nuclear angular moments decouple, so that $I$ and $J$ act independently, giving projections $m_j$ and $m_i$ on the field vector.

### 11.6.2. *Atomic beams*

The hyperfine spectra are obtained from light sources in the absence of any external (to the atom) magnetic field. If the source is placed between the poles of a magnet, whose strength $B$ is progressively increased, the following sequence of changes takes place (see Table 11.2, electron-nucleon interaction).

Suppose $B$ is increased slowly to $10^{-2}$ T. Each hyperfine level $F$ is found to split into $2F + 1$ levels, since the quantum mechanical rule of permitted projections on an external field vector comes into operation. These permitted projections can vary from zero to a maximum value of $F$; for $F = 3$ seven new lines are obtained. Further increases in $B$ to 10 T leads to a decoupling of $F$ into its components $J$ and $I$ (Fig. 11.10). For each projection of $J$ on the field vector there are $2I + 1$ lines ($-I \ldots 0 \ldots +I$), giving altogether $(2J + 1)(2I + 1)$ lines. The splitting of the spectral lines in a weak magnetic field is called the *Zeeman effect*.

The decoupling of the angular momentum of the atom into its electronic and nuclear components is used in the *atomic beam apparatus* to determine nuclear magnetic moments and spin values. A beam of atoms, produced in an oven, is allowed to enter a tube along which a series of magnets (usually three) have been placed. The magnetic field splits the atomic beam into several component beams, each containing only atoms which have the same values for all the quantum numbers. Between the magnets there is a small coil connected to a high frequency oscillator, which produces a weak oscillating magnetic field. When this oscillator is tuned to an energy $\mathbf{h}\upsilon$, which exactly matches the energy difference between two quantum states of the atom, energy may be absorbed producing a transition from one of the states to another. Subsequently the atoms are deflected differently by the magnetic field than they were before the energy absorption. By a combination of homogeneous and heterogeneous magnetic fields the atomic beam apparatus allows only those atoms which have absorbed the energy quantum $\mathbf{h}\upsilon$ to reach the detector. From the

properties of the magnetic fields and the geometric dimensions and frequency of the instrument, the magnetic moment of the atom in different quantum states can be determined. This allows calculation of the magnetic moment and spin of the nucleus. This technique is of interest to the nuclear chemist because spin values can be obtained for short-lived nuclei in submicroscopic amounts. In contrast the hfs technique requires macroscopic amounts of atoms.

### 11.6.3. *Nuclear magnetic resonance*

When an atom is placed in an external magnetic field (strength $B$) so that $J$ and $I$ decouple (cf. (11.31)), the nuclear magnetic moment vector $\boldsymbol{\mu}_I$ must precess around the field direction, with the components in the direction of the field restricted to

$$\mu_I = g_I \mathbf{B}_n m_I \tag{11.32}$$

In the external field the states with different $m_I$ have slightly different energies. The potential magnetic energy of the nucleus is

$$E_{magn} = -\boldsymbol{\mu}_I B = -g_I \mathbf{B}_n m_I B \tag{11.33}$$

The energy spacing between two adjacent levels is:

$$\Delta E = g_I \mathbf{B}_n B \tag{11.34}$$

because $\Delta m_I = \pm 1$. For example, consider the case of the nucleus $^{19}$F for which $g_I = 5.256$ in a field of 1 T, $\Delta E = 5.256 \times 5.0505 \times 10^{-27} \times 1 = 2.653 \times 10^{-26}$ J. The frequency of electromagnetic radiation corresponding to this energy is $4.0 \times 10^7$ s$^{-1}$ or 40 MHz. This lies in the short wave length region, $\lambda = 7.5$ m. This frequency is also the same as that of the Larmor precession, as given by (11.24b).

These relations can be used to calculate the nuclear magnetic moment, if $I$ is known, or vice versa. Figure 11.11 shows the results of an experiment in which a sample has been placed in a variable magnetic field containing two coils, one connected to a radio transmitter operating at 5 MHz and the other to an amplifier. The sample is a glass tube (B, O, Na, Al, Si atoms) containing a piece of copper alloy (Cu, Al) in water (H, D, O). By varying the magnetic field a number of resonances are observed. For example, for $^{23}$Na one has a resonance at 0.443 T. With (11.34) we can calculate $g_I = 1.48$, and, consequently, the magnetic moment of $^{23}$Na is 2.218 (Table 11.3). Further, for $^{23}$Na, $m_I = 3/2$ and $I = 3/2$.

The magnetic field experienced by the nucleus is not exactly equal to the external field because of the shielding effect of the electron shell, even if $I$ and $J$ are decoupled. Although this shielding of the nucleus is very small, about $10^{-5}$ B, it can still easily be detected with modern equipment. The shielding effect depends on the electronic structure.

The structural information that can be provided by this method is very detailed, and a new and deeper insight in chemical bonding and molecular structure is provided. The nmr technique has therefore become a central tool for the investigation of chemical structures

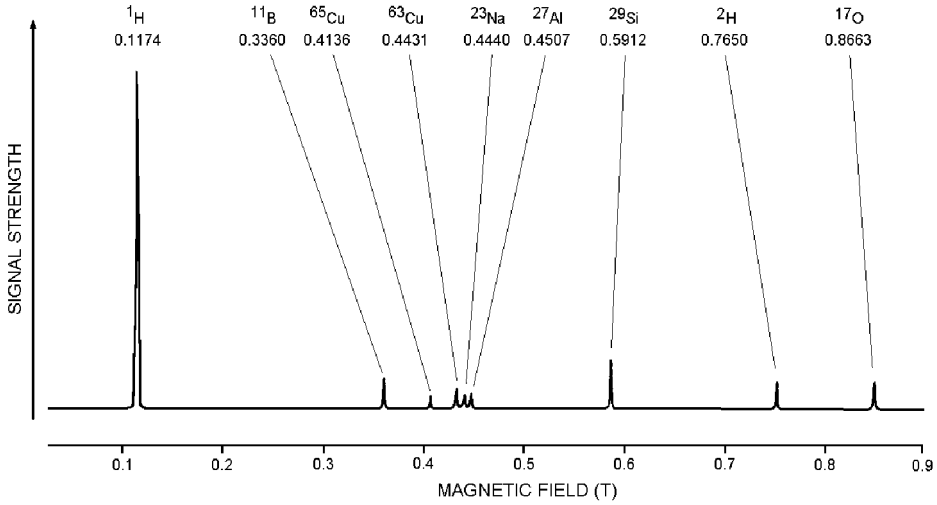


FIG. 11.11. Nmr spectrum for a glass vessel containing water and some copper. The magnetic field is given in tesla (T).

in solids, liquids, and the gaseous state. Tomography by nmr is also a valuable tool for medical imaging.

## 11.7. Radioactive decay and nuclear structure

In the preceding section we have described three methods of determining nuclear spin – one optical and two magnetic. The nuclear spin plays a central role in forming the nuclear energy states. It is therefore to be expected that it also should be of importance in nuclear reactions and in radioactive decay. Let us consider some rules for the lifetimes of unstable nuclei, for their permitted modes of decay, and for the role of nuclear spin. Knowing these rules, it is, for example, possible from a decay scheme to predict the spin states of levels which have not been measured.

### 11.7.1. *Gamma-decay*

Photons are emitted in the transition of a nucleus from a higher energy state (level) to a lower

$$E_\gamma = \mathbf{h}\upsilon = E_f - E_i \tag{11.35}$$

where f and i refer to the final and initial states. Because the photon has spin 1, de-excitation through γ-emission is always accompanied by a spin change $\Delta I$ 1. This leads to a change in the charge distribution of the nucleus and hence also to a change in its magnetic properties. Depending on the type of change occurring through the γ-emission, the radiation is classified as electric or magnetic (§11.4) according to the scheme in the left part of Table 11.7. Although parity need not be conserved in γ-decay, the parity change

TABLE 11.7. *Classification of radiation emitted in γ-decay and lifetime calculations of the excited states for given γ-energies* (From Blatt and Weisskopf.)

| Type of radiation | Name of transition | Spin change $\Delta I = \Delta l$ | Parity change | Average lifetime (τ) in seconds for γ-energy level | | |
|---|---|---|---|---|---|---|
| | | | | 1MeV | 0.2 MeV | 0.05MeV |
| E1 | Electric dipole | 1 | Yes | $4\times10^{-16}$ | $5\times10^{-14}$ | $3\times10^{-12}$ |
| M1 | Magnetic dipole | 1 | No | $3\times10^{-14}$ | $4\times10^{-12}$ | $2\times10^{-10}$ |
| E2 | Electric quadrupole | 2 | No | $2\times10^{-11}$ | $6\times10^{-8}$ | $6\times10^{-5}$ |
| M2 | Magnetic quadrupole | 2 | Yes | $2\times10^{-9}$ | $5\times10^{-6}$ | $5\times10^{-3}$ |
| E3 | Electric octupole | 3 | Yes | $2\times10^{-4}$ | 2 | 70 h |
| M3 | Magnetic octupole | 3 | No | $2\times10^{-2}$ | 180 | 200 d |

associated with the different types of γ-transitions is listed in that table.

Based on the single-particle model, Blatt and Weisskopf have calculated probable lifetimes for excited states assuming a model nucleus with a radius of 6 fm. For $2^L$-multipole transitions of electric (E) or magnetic (M) type they derived the following equations

$$\lambda_{EL} = 4.4\times10^{21}\{(L+1)/[L((2L+1)!!)^2]\}\{3/(L+3)\}^2(E_\gamma/197)^{(2L+1)}r^{2L} \qquad (11.36a)$$

$$\lambda_{ML} = 1.9\times10^{21}\{(L+1)/[L((2L+1)!!)^2]\}\{3/(L+3)\}^2(E_\gamma/197)^{(2L+1)}r^{2L-2} \qquad (11.36b)$$

where $L$ is the angular momentum carried away by the photon ($= \Delta l$), $\lambda$ is the decay constant in $s^{-1}$, $E\gamma$ is the γ-ray energy in MeV and $r$ is the nuclear radius in fm.

As seen, for decay involving electric multipole transitions the average lifetime τ is proportional to $r^{-2\Delta l}$, and for decay involving magnetic multipoles, to $r^{-2(\Delta l-1)}$; in the decay the nuclear spin quantum number $s$ does not change. Calculated values are included in Table 11.7.

The decay of $^{24m}$Na ($I = 1+$) to $^{24}$Na ($I = 4+$) provides a useful example. The transition involves $\Delta l = 3$, no (i.e. there is no parity change), so it is designated as M3. The γ-energy is 0.473 MeV and the nuclear radius of $^{24}$Na is about 3.7 fm. In order to compare this energy with those given in Table 11.7, a radius correction from the assumed 6 fm to the observed 3.7 fm must be made; accordingly $E_{corr} = E_{obs}(r_i/6)^{-2(\Delta l-1)}$ for M-type radiation. This gives a hypothetical energy of $0.473(3.7/6)^{-4} = 3$ MeV. According to Table 11.7 the lifetime should be $> 0.02$ s; the observed value is 0.035 s. The agreement between experiment and calculation is sometimes no better than a factor of 100.

The Blatt-Weisskopf relationship between energy and lifetime is only applicable for excited nucleonic states, not for rotational states. In the decay of these states the rotational quantum number always changes by two units and the lifetime of the states is proportional to $E_\gamma^{-5}Q^{-2}$. The lifetimes are so short that no rotationally excited isomers have been observed as yet.

### 11.7.2. *Beta-decay*

Beta-decay theory is quite complicated and involves the weak nuclear interaction force, which is less understood than the strong interaction. The theory for β-decay derived by Fermi in 1934 leads to the expression

$$\lambda = G M^2 f \tag{11.37a}$$

for the decay constant, λ. $G$ is a constant, $M$ is the nuclear matrix element describing the change in the wave function during the β-transformation (i.e. of a proton into a neutron for positron emission, or the reverse for negatron emission), $f$ is a function of $E_{max}$ and $Z$. $M$ depends on the wave functions before and after the transformation and gives the "order" of decay. Since $t_{½} = \ln 2/\lambda$

$$\ln 2 = G M^2 f t_{½} \tag{11.37b}$$

we see that the product $ft_{½}$ should be constant for a decay related to a certain $M$. The $ft$ value (omitting index ½) is often referred to as the comparative β half-life, and nomograms for its calculation are given in nuclear data tables and decay schemes. The lower the $ft$ value the higher is the probability for decay, and the shorter is the half-life. Gamow and Teller have given selection rules for β-decay which are useful for estimating decay energy, half-life, or spin in a certain decay process, if two of these properties are known. These rules are summarized in Table 11.8.

For example, the decay of $^{24}$Na occurs 99% through β-emission (with an $E_{max} = 1.4$ MeV) to an excited state of $^{24}$Mg (Fig. 4.7). The log $ft$ value of the transition is 11.1. The ground state of $^{24}$Mg is $0+$; the excited state has positive parity. Thus the selection rules indicate an allowed transition for which the only spin changes permitted are 0 and $\pm 1$. The ground state of $^{24}$Na is $4+$, and the observed excited state (at the 4.12 MeV level) is $4+$, in agreement with the rule.

### 11.7.3. *Alpha-decay theory*

If we calculate the $Q$-value for the α-decay reaction (4.11) from the mass formulae (4.12) we find that $Q > 0$ for all nuclei with $A > 150$, which means that we would expect all elements heavier than the rare earths to be unstable with respect to α-decay. However, the accuracy of eqn. (3.8) decreases when we move away from the region of β stability. Hence, we should not be surprised that nuclides, with a high $Z/A$ ratio, far from stability have been found to decay by α-emission down to $A = 106$. For nuclei nearer β-stability, decay by emission of α-particles is observed for some isotopes of rare earths and heavier elements, but it occurs frequently only for $A \quad 210$, i.e. nuclides heavier than $^{209}$Bi.

In §4.17 we mentioned the discovery by Geiger and Nuttall that the lower the α-energy the longer was the half-life of the α-decay; doubling the decay energy may reduce the half-life by a factor of $10^{20}$. Alpha-decay has been observed with energies from slightly greater than 1.8 MeV (e.g. $^{144}$Nd, $E_\alpha = 1.83$ MeV, $t_{½} = 2.1 \times 10^{15}$ y) to about 10 MeV (e.g. $^{262}$Ns, $E_\alpha = 10.38$ MeV, $t_{½} = 4.7$ ms). The isotopes of the actinide elements typically

TABLE 11.8. *Gamow–Teller selection rules for* β*-decay*

| Transition type | $\Delta I$ | Parity change | Log *ft* |
|---|---|---|---|
| Super allowed | 0 | No | 3 |
| Allowed | $0, \pm 1$[(a)] | No | 4-6 |
| First forbidden | $0, \pm 1, \pm 2$ | Yes | 6-9 |
| ond forbidden | $\pm 2, \pm 3$[(b)] | No | 10-13 |

[(a)]Not 0 0, [(b)]Also 0 0.

have α-energies between 4 and 10 MeV.

The observed stability against α-decay for most nuclei in the range 102 $A$ 210 having a positive $Q_\alpha$ can be explained by assuming the α-particle exists as a (preformed) entity inside the nucleus but with insufficient kinetic energy to overcome the "internal Coulomb barrier". This barrier is assumed to be of the same type, although of somewhat different shape, as the external Coulomb barrier, which is discussed in some detail in §12.4.

Assume that the average kinetic energy is at the level marked $E_\alpha$ in Figure 11.12. If the particles in the nucleus have a Boltzmann energy distribution, an α-particle could in principle form in the nucleus and perhaps acquire sufficient kinetic energy through collisions to overcome the barrier ($E_{cb}$). It would then be emitted with an energy $E_{cb}$, which for an element like uranium is 26 MeV. However, the observed α-energy is only 4.2 MeV.

This contradiction was explained by Gamow, and independently by Gurney and Condon, in 1928, by using a quantum mechanical model, which retained the feature of the "one-body model" with a preformed α-particle inside the nuclear potential wall of even-even nuclei.

The time independent solution to the Schrödinger wave equation for an α-particle inside the nuclear potential well is a wave function which has a small, but non-zero, value even outside the potential well. The probability, $p$, to find the α-particle outside the potential well is the square of the wave function and is found to be

$$p = \exp\left[-\{4\pi(2\mu)^{1/2}/\mathbf{h}\} \int_{R}^{R_x} (U(r)-Q_\alpha)^{1/2}\, dr\right] \qquad (11.38)$$

where index α refer to the α-particle, μ is the reduced mass of α-particle and residual nucleus, $\mu = M_\alpha M_1/(M_\alpha + M_1)$, $R$ and $R_x$ are inner and outer integration limits respectively (where the potential energy of the barrier is equal to the energy of the emitted particle, cf. Fig 11.12), $r$ is the distance from the center of the nucleus, $U(r)$ is the potential energy of the α-particle, and $Q_\alpha$ is the total α-decay energy. Index 1 refer to the nucleus remaining after emission of the α-particle.

The decay constant can be regarded as the product of $p$ and the frequency, $f$, by which the α-particle hits the barrier from inside. If we assume that the deBroglie wavelength, $\mathbf{h}/\mu v$, for an α-particle of velocity $v$ inside the nucleus is approximately equal to the nuclear radius, $R$, we obtain

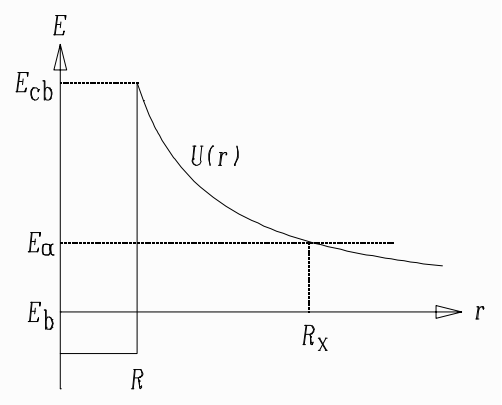


FIG. 11.12. Alpha-penetration through the potential wall.

$$\mathbf{h}/\mu v \quad R \tag{11.39}$$

The frequency $f$ can then be estimated from $v$ if we assume that the α-particle bounces back and forth inside the potential well with constant velocity.

$$f = v/2R \quad \mathbf{h}/2\mu R^2 \tag{11.40}$$

Combining (11.40) with (11.38) we obtain the following expression for the decay constant

$$\lambda \quad [\mathbf{h}/(2\mu R^2)] \exp\{-[4\pi(2\mu)^{1/2}/\mathbf{h}] \int_R^{R_x} (U(r)-Q_\alpha)^{1/2}\, dr\} \tag{11.41}$$

The same relation also holds – with appropriate substitutions – for any charged particle trying to enter the nucleus from outside the potential barrier (cf. §12.4), where, however, only one impact is possible, i.e. $f = 1$.

For some simple mathematical forms of the potential energy $U(r)$ it is possible to find analytical solutions to the integral in (11.41). The simplest form of $U(r)$, a square well nuclear potential according to Figure 11.12, yields the following expression after integration and some algebra[1]

$$\lambda \quad [\mathbf{h}/(2\mu R^2)] \exp\{-[(2\mu)^{1/2}\mathbf{e}^2 Z_1 Z_\alpha /(\ _0 \mathbf{h} Q_\alpha^{1/2})][\arccos(u)-u(1-u^2)^{1/2}]\} \tag{11.42}$$

where

$$u = (E_\alpha/E_{cb})^{1/2} = [4\pi\ _0 Q_\alpha R/(Z_1 Z_\alpha \mathbf{e}^2)]^{1/2} \tag{11.43}$$

The radius of the decaying nucleus can be estimated from

[1] It is important to recognize the difference between the classical CGS system where the force $F$ between point charges in vacuum is $F = z_1 z_2 \mathbf{e}^2/r^2$ and the SI system where $F = z_1 z_2 \mathbf{e}^2/(4\pi\ _0 r^2)$.

$$R = r_0 A_1^{1/3} + r_\alpha \quad 1.30\, A_1^{1/3} + 1.20 \ \text{(fm)} \tag{11.44}$$

where $A_1$ is the mass number of the nucleus after emission of the α-particle and $r_\alpha$ is the effective radius of the α-particle. Equation (11.42) can not only be used to compute decay constants, but also to estimate the nuclear radius for even-even α-emitters from measured half-lives and decay energies. The calculated decay constant is very sensitive to $Q_\alpha$: a 1 MeV increase in $Q_\alpha$ increases λ (and decreases $t_{½}$) by a factor of about $10^5$. It is also very sensitive to the nuclear radius: a 10% increase in $R$ (or the Coulomb radius $r_c$; see Fig. 12.4) which means a corresponding decrease of the Coulomb barrier height, increases λ by a factor of 150.

Decay constants and partial α half-lives computed from (11.42) are normally within a factor 4 of the measured values for even-even nuclei. The half-lives of even-odd, odd-even, and odd-odd nuclides are often longer than predicted by equations like (11.42), even after

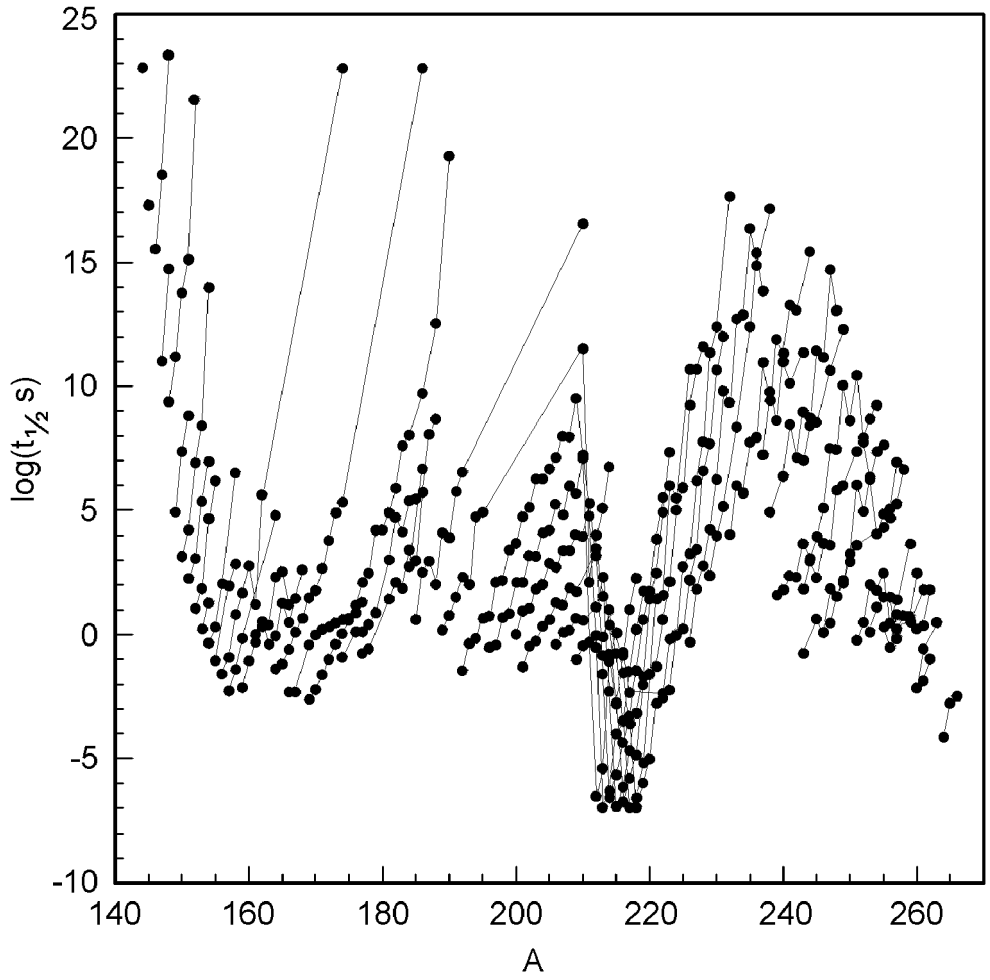


FIG. 11.13. The variation of α-half-life with mass number. Lines connect isotopes.

inclusion of more elaborate nuclear potentials and angular momentum effects in the theory. The ratio between the observed and predicted half-lives is called *hindrance factor* and ranges from one to ~3000.

Assuming the Coulomb barrier to be much larger than $Q_\alpha$, i.e. $u$ small, designating the resulting exponential term in (11.42) by $e^{-2G}$ and taking the logarithm of the resulting expression we obtain

$$\log \lambda = \text{constant} - 2G \tag{11.45}$$

which is very similar to the empirical Geiger-Nuttall law.

Figure 11.13 shows the systematic change of α-decay half-life with nuclear charge and mass for heavy nuclei, lines connect data for constant $Z$. Odd-even effects and influence from magic numbers are visible. Such diagrams have historically played an important role in the synthesis and identification of isotopes of the heaviest elements.

The α-decay theory was the first successful (quantum mechanical) explanation of radioactive decay, and as such played a major role in further development of nuclear theories and models. Although its simplicity causes it to fail for nonspherical nuclei as well as those near closed shells, such effects can be taken into account in more advanced Nilsson-type calculations.

### 11.7.4. *Spontaneous fission*

In §4.4 we found that fission of heavy nuclei like $^{236}$U is exoergic and in §4.6 that it is a common decay mode for the heaviest nuclei. From the semiempirical mass equation (3.8) it can be found that fission of nuclei with $A \quad 100$ have positive $Q$-values. Why is the decay by spontaneous fission only observed for nuclei with $A \quad 230$?

The breakup of a large even-even nucleus into two positively charged fragments of roughly equal mass and charge can be treated in a way similar to that of α-decay. Assuming separation into two spherical fragments, $A_1$ $Z_1$ and $A_2$ $Z_2$, in point contact the Coulomb energy can be calculated to be

$$E_{cb} = 0.96\, Z_1 Z_2 / (A_1^{1/3} + A_2^{1/3}) \ \text{(MeV)} \tag{11.46}$$

where $r_0 = 1.5$ fm has been assumed. In a real case it is necessary to consider that the newly formed fragments have non-spherical shapes and the value obtained from (11.46) is thus very approximate but sufficient for our discussion. The spontaneous fission of a nucleus is obviously hindered by a Coulomb barrier, the *fission barrier*, and the process should be treated as a barrier penetration problem for $Q < E_{cb}$. When $Q \quad E_{cb}$, breakup of the nucleus will occur within a few nuclear vibrations, $\sim 10^{-22}$ s.

The critical condition $Q = E_{cb}$ for fission of an even-even nucleus into two equal fragments with an unchanged charge to mass ratio can be estimated by equating $E_{cb}$ from (11.46) with the $Q$-value computed from (3.8). Neglecting the pairing term this results in

$$(Z^2/A)_{crit} = 37.89 \tag{11.47a}$$

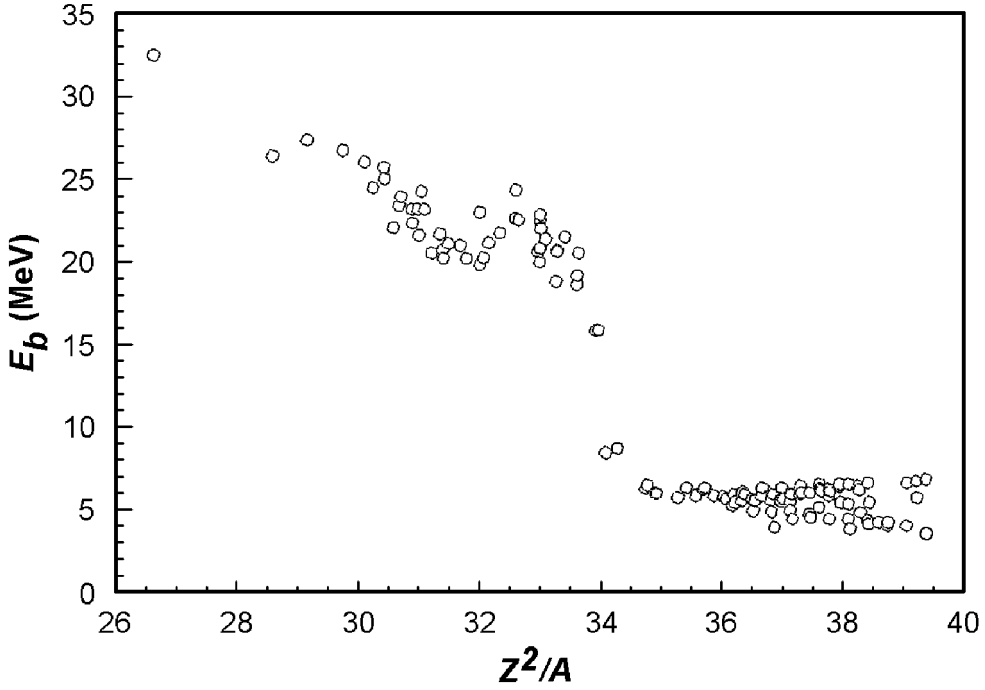


FIG. 11.14. Fission barrier height as function of $Z^2/A$.

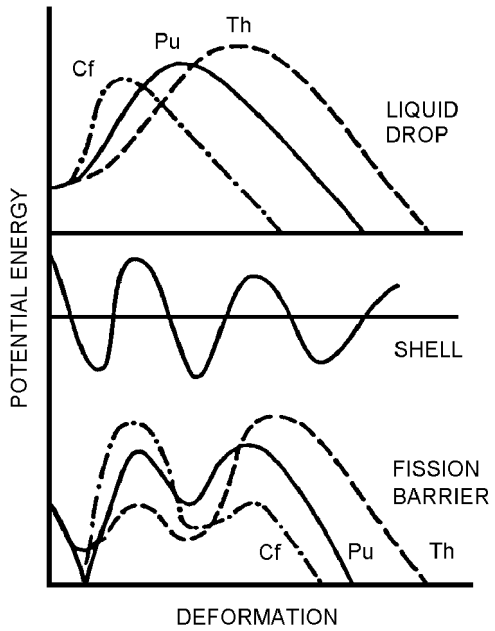


FIG. 11.15. Qualitative features of the fission barrier for Pu (From Britt).

Because asymmetric fission is more common than symmetric and the emerging fission fragments have non-spherical form, the numerical value derived above is not very accurate. However, the concept of a critical value of $Z^2/A$ is important. A more sophisticated treatment results in the equation

$$(Z^2/A)_{crit} = 50.883\,[1 - 1.7826\,(N - Z)^2/A^2] \qquad (11.47b)$$

We can then define a *fissionability parameter*, $x$,

$$x = (Z^2/A)/(Z^2/A)_{crit} \qquad (11.48)$$

as a measure of how prone to fission a nucleus is.

Figure 11.14 shows fission barrier height as function of $Z^2/A$. Calculations by Myers and Swiatecki using a refined liquid drop model predict that the barrier height should pass through a maximum around $Z^2/A \sim 16$. The penetrability of the barrier increases roughly exponentially with its height. Hence, low values of $Z^2/A$ (but above the value corresponding to the maximum barrier height) implies extremely long half-lives. As an example, $^{238}$U has $Z^2/A = 35.56$, $E_{cb} = 5.8$ and a partial half-life for spontaneous fission, $t_{½,SF}$, of $\sim 10^{16}$ y. By comparison we can estimate that a nucleus with $A = 100$ and $Z = 44$ ($^{100}$Ru), $Z^2/A = 19.36$, has a fission barrier tens of MeV high and a practically infinite half-life with regard to spontaneous fission.

So far we have neglected the effects of pairing, nuclear shell structure and nuclear deformation on the fission process. Odd-even, even-odd and odd-odd nuclei exhibit large hindrance factors, HF, for spontaneous fission somewhat similar to the phenomenon observed in α-decay. The presence of one or two odd nucleons leads to spin and parity values which must be conserved during the deformations leading to fission and thus constrains the possible shapes and energy levels. This contributes to the occurrence of hindrance factors. Hence, o-e, e-o and o-o nuclei have normally much longer spontaneous fission half-lives than their neighboring e-e nuclei.

The ground state energy, $E$, of a nucleus can be regarded as a sum of the liquid drop model energy (including deformation), $E_{LDM}$, the pairing correction, $_P$, and the shell correction, $_S$, to that energy.

$$E = E_{LDM} + {}_P + {}_S \qquad (11.49)$$

The use of (11.49), with deformation dependent shell corrections, leads to fission barriers with two maxima, see Figure 11.15. The occurrence of a secondary minimum is consistent with the observation of spontaneous fission isomers. Shell and pairing effects also give rise to long spontaneous fission and α-decay half-lives for nuclides around magic $N$ or $Z$ numbers. Detailed calculations based on advanced theories of nuclear structure lead to the prediction of an area of spheroidal nuclei with increased nuclear stability (in their ground state) around $Z = 114$ and $N = 184$, the so called *superheavy elements*. However, attempts to synthesize such nuclei in their ground state by heavy ion reactions have been fruitless.

## 11.8. Exercises

**11.1.** The quantum numbers $s = 1/2$ and $l = 2$ are assigned to a particle. (a) If spin and orbital movements are independent, how many space orientations (and thus measured spectral lines if no degeneration of energy states occur) are possible in an external field of such a strength that both movements are affected? (b) How many lines would be observed if spin and orbital movements are coupled?

**11.2.** In the hydrogen atom the K-electron radius is assumed to be $0.529 \times 10^{-10}$ m (the Bohr radius). (a) Calculate the orbital velocity of the electron assuming its mass to be $\mathbf{m}_e$. (b) How much larger is its real mass because of the velocity? Does this affect the calculations in (a)?

**11.3.** A beam of protons pass through a homogeneous magnetic field of 0.5 T. In the beam there is a small high frequency coil which can act on the main field so that the proton spin flips into the opposite direction. At which frequency would this occur?

**11.4.** Calculate the nuclear Landé factor for $^{11}$B.

**11.5.** In Table 11.5 the first degenerate levels have been given. Using the same assumptions, what states will be contained in the next level and how many nucleons will it contain?

**11.6.** How deep is the nuclear well for $^{116}$Sn if the binding energy of the last nucleon is 9 MeV?

**11.7.** Calculate the spins and nuclear *g* factors for (a) $^{45}$Ca, (b) $^{60}$Co, and (c) $^{141}$Pr, using data in Table 11.3.

**11.8.** The observed quadrupole moment of $^{59}$Co is 0.40 barn. (a) What is the deformation value $\beta$? (b) What spin value is expected from the Nilsson diagram?

**11.9.** Which neutron and proton states account for the spin value *I* of $^{14}$N?

**11.10.** A $\gamma$-line at 0.146 MeV is assigned to a $+4 \quad +0$ rotational level change in $^{238}$Pu. (a) What should the energy of the $+2$ and $+6$ rotational levels be? Compare with the measured values of 0.044 and 0.304 MeV. (b) If $^{238}$Pu is considered to be a homogenous sphere, what will its apparent radius be? Compare with that obtained using relation (3.7).

**11.11.** A $^{239}$Pu compound is placed in a test tube in a 40 MHz nmr machine. At what field strength does resonance occur with the nuclear spin? Is the measurement possible? Relevant data appear in Table 11.3.

**11.12.** Using the Gamow theory the probability for tunneling of an $\alpha$-particle in the decay of $^{238}$U is $1{:}10^{38}$, and the $\alpha$-particle hits the walls about $10^{21}$ times per second. What average lifetime can be predicted for $^{238}$U from this information?

**11.13.** Calculate the half-life for $\alpha$-decay of $^{147}$Sm assuming that $Q_\alpha$ is 2.314 MeV. Compare the result with the measured half-life and compute the hindrance factor.

## 11.9. Literature

I. PERLMAN, A. GHIORSO, and G. T. SEABORG, Systematics of alpha-radioactivity, *Phys. Rev*. 77 (1950) 26.
I. PERLMAN and J. O. RASMUSSEN, Alpha radioactivity, *Handbuch der Physik* 42, Springer-Verlag, 1957.
W. J. MOORE, *Physical Chemistry*, 3rd edn., Prentice-Hall, I. 1962.
W. D. MYERS and W. J. SWIATECKI, Nuclear Masses and Deformations, *Nuclear Physics* **81** (1966) 1.
E. K. HYDE, Nuclear models, *Chemistry* 40 (1967) 12.
H. C. BRITT, in N. M. EDELSTEIN (Ed.), *Actinides in Perspective*, Pergamon, 1982, p. 245.
K. S. KRANE, *Introductory Nuclear Physics*, Wiley, 1988.
G. T. SEABORG and W. D. LOVELAND, *The Elements Beyond Uranium*, Wiley-Interscience, 1990.
D. N. POENARU (Ed.), *Handbook of Decay Modes*, CRC Press, 1993.